Research Square

Preprints are preliminary reports that have not undergone peer review.
They should not be considered conclusive, used to inform clinical practice,
or referenced by the media as validated information.

Expert-Guided Multimodal EEG–ECG Integration for Long-Term Neurological Outcome Prediction After Cardiac Arrest

Calixto Machado

cmachado_2000@yahoo.com

Institute of Neurology and Neurosurgery, Havana

Beata Drobná Sániová

Comenius University Bratislava

Michal Drobný

Comenius University Bratislava

Raed Mualem

The Edmond J. Safra Brain Research Center for the Study of Learning Disabilities, University of Haifa,

---

Research Article

Keywords: Cardiac arrest, multimodal neurophysiology, cortical dynamics, heartbeat-evoked responses, heart-rate variability, EEG microstates, neuroprognostication

Posted Date: November 18th, 2026

DOI: https://doi.org/10.21203/rs.3.rs-11651809/v1

License: This work is licensed under a Creative Commons Attribution 4.0 International License.
Read Full License

Additional Declarations: No competing interests reported.

Abstract

Objectives

To investigate whether integrating complementary cortical and cardiovascular neurophysiological biomarkers improves the characterization and internal prediction of neurological outcomes following cardiac arrest.

Background

Recovery after postanoxic coma involves cortical network organization, nonlinear cerebral dynamics, autonomic regulation and brain-heart communication. Multimodal neurophysiology offers a more comprehensive perspective than isolated measurements.

Methods

We analyzed 134 outcome-labeled post-cardiac-arrest coma records; 121 had complete predictors (48 favorable, 73 poor). The corresponding author (C.M.) performed expert visual EEG/ECG curation incorporating ICA-based artifact management. M2 comprised age, relative alpha/theta power and Hilbert-Huang complexity; M3 additionally incorporated frontal heartbeat-evoked responses (HER) and heart-rate variability (SDHR). Elastic Net, Gradient Boosting and within-fold algorithm selection were evaluated with repeated nested five-fold cross-validation.

Results

Gradient Boosting achieved an out-of-fold AUC of 0.738 for M3 versus 0.713 for M2 (difference 0.025; exploratory 95% CI -0.051 to 0.104). Nested selection yielded AUCs of 0.709 and 0.654, respectively (difference 0.055; 95% CI -0.022 to 0.135). Both incremental intervals included zero.

Conclusions

Expert-guided multimodal EEG-ECG integration offers a complementary framework for evaluating cortical function and brain-heart interactions. Internal discrimination was moderate; added predictive value of HER and HRV remains uncertain and requires independent validation.

INTRODUCTION

Neurological injury is a central determinant of disability after successful resuscitation from cardiac arrest. The prognostic problem is difficult because an apparently unresponsive patient may still be

exposed to sedative medication, temperature management, systemic instability and evolving cerebral injury. Contemporary recommendations emphasize a delayed, integrated assessment rather than interpretation of a single early electrophysiological test. Neurological outcome studies must also account for the possibility that pessimistic prognoses influence withdrawal of life-sustaining treatment, creating a self-fulfilling association between a marker and death [1,2,3,4,5].

The International Cardiac Arrest Research (I-CARE) initiative offers unusually rich longitudinal electroencephalography (EEG), electrocardiography (ECG) and outcome information from multiple institutions. Resources of this kind expand access to physiologically meaningful recordings beyond the hospitals where they were collected and promote independent computational analyses [6,7]. Yet a public or shared database is not an independently certified collection of artifact-free biosignals. Original acquisition, electrode integrity, signal synchronization, intensive-care interventions and annotation practices can differ between sites. These issues are more consequential when a derived predictor is a small stimulus-locked voltage fluctuation or a beat-to-beat rhythm statistic.

Shared physiological repositories permit independent hypothesis-driven research, but their re-use requires careful attention to methodological originality, signal quality and transparent analysis. Expert-supervised curation and a biologically motivated multimodal question can extend the value of such resources [6,7,8,9,10].

Continuous EEG offers direct access to cortical electrical activity and its evolution during postanoxic recovery. Quantitative spectral features can capture changes in slowing, alpha preservation and other aspects of background organization. However, they remain vulnerable to sedation, technical noise and changes in muscle activity; expert EEG interpretation continues to add context that automated feature pipelines cannot infer reliably from numerical tables alone [11,12,13,14,15,16,17,18,19].

Nonlinear EEG dynamics add a different signal description. The Hilbert–Huang transform decomposes nonstationary activity into adaptive modes and provides instantaneous-frequency representations, motivating complexity indices that may quantify residual cortical organization [20]. The physiological meaning of any specific entropy or complexity metric nevertheless depends on its filtering, epoch selection, normalization and artifact handling. A number is not interchangeable with a clinician’s interpretation of an EEG background.

Heartbeat-evoked responses (HER) represent EEG activity time-locked to cardiac events and have been investigated in interoception, consciousness and disorders of consciousness. Their possible value after global ischemia is compelling: severe brain injury affects both cerebral dynamics and the integration of ascending physiological signals. Conversely, a heartbeat-locked scalp voltage can arise from the spread of the cardiac field, ECG contamination, or movement; temporal coupling alone does not imply a cortical source [21,22,23,24].

Heart-rate variability (HRV) describes variation in cardiac intervals, with established quantitative conventions and known dependence on rhythm regularity and observation length. Ectopic beats,

resuscitation arrhythmias and imperfect R-peak detection may change variability estimates without reflecting autonomic neural function. Nonlinear or Hilbert–Huang treatments of heart-rate time series similarly require clear quality criteria and a well-defined physiological interpretation [25,26,27,28].

EEG microstates provide a complementary representation of rapidly changing scalp topographies and potentially link distributed neuronal processes with the timing of autonomic events. Their interpretation is vulnerable to low-amplitude background activity, algorithmic configuration and missingness in profoundly suppressed recordings. Their presence in a broader conceptual framework does not establish additional predictive benefit in the present analytic cohort [29,30,31,32].

The rationale for multimodal monitoring is that neurological recovery after cardiac arrest cannot be characterized fully by one electrophysiological dimension. Quantitative EEG captures cortical spectral organization, and the Hilbert-Huang transform describes nonlinear and nonstationary dynamics. Heartbeat-evoked responses investigate cortical activity related in time to cardiac events, while heart-rate variability describes cardiovascular rhythm regulation. EEG microstates add a network-level view through rapidly evolving scalp topographies. Together, these domains provide a complementary physiological framework for studying cortical integrity, brain-heart interactions and recovery of consciousness. Microstate organization may be relevant to rehabilitation after coma, although its prognostic contribution was not established in the present model.

We assessed whether an integrative, physiologically informed set of cortical and cardiac biomarkers can discriminate neurological outcome after cardiac arrest. The four-feature set (M2) comprised age, alpha/theta EEG power and Hilbert-Huang complexity, and the six-feature set (M3) additionally included frontal HER and SDHR. We also discuss microstate organization as a complementary, exploration domain of cortical network assessment, without attributing the M3 model results to microstate features.

MATERIALS AND METHODS

Study design, clinical outcome and analytical samples

This retrospective secondary analysis used a locally assembled set of I-CARE-derived EEG, ECG and outcome features. In the working master table, 134 post-cardiac-arrest coma records carried an outcome label: 52 favorable (Cerebral Performance Category [CPC] 1–2) and 82 poor (CPC 3–5). In the consortium, the CPC was ascertained at three to six months, depending on the participating institution [6]. The present analysis used the outcome categories stored in the derived table.

Of 134 records, 121 had all six features required by the primary comparisons (48 favorable and 73 poor). A nested subset of 104 (43 favorable and 61 poor) additionally had selected microstate-coverage variables. These groups indicate analytical feature availability; they do not establish a prospective screening flow or clinical reasons for individual missing values. Figure 1 and Table 1 show their characteristics.

Table 1
Analytical cohorts and predictor sets

Analytical cohort	N	Favorable	Poor	Predictor availability
Available coma records	134	52	82	Outcome available
M3 complete cases	121	48	73	Age, alpha, theta, HHT, frontal HER, SDHR
M3 + selected microstates	104	43	61	M3 variables + selected microstate coverage

Note. Cohort sizes describe feature availability. Specific causes of missing measurements were not independently verified.

Expert-Supervised Data Curation and Neurophysiological Quality Control

A major methodological strength of the present study is integrating expert neurophysiological assessment with computational signal processing and multimodal predictive modeling. Unlike approaches that rely exclusively on automated feature extraction from publicly available databases, the original EEG and ECG recordings underwent expert-guided curation by the corresponding author (C.M.), an experienced clinical neurophysiologist.

This process incorporated visual inspection of electrophysiological recordings, assessment of signal integrity, identification of physiological and technical artifacts, and independent component analysis (ICA) to address non-neural contamination of EEG signals, particularly cardiac field artifacts that may interfere with heartbeat-evoked responses. We also paid particular attention to ECG signal quality and identified rhythm disturbances that could affect HRV measurements.

The combination of expert visual assessment, ICA-based signal processing, and multimodal integration of cortical, nonlinear, and cardiovascular biomarkers represents an important methodological contribution. By incorporating clinical neurophysiological expertise into the analytical workflow, the study extends beyond conventional automated database mining and provides a physiologically informed framework for investigating neurological outcomes after cardiac arrest.

This expert-guided approach is especially valuable in studies using shared physiological databases, where appropriate signal interpretation and artifact management are essential to obtain meaningful, clinically interpretable results.

Predictor definitions and neurophysiological rationale

The base feature set (M2) comprised age, alpha_rel, theta_rel, and HHT_Complexity_x. Relative alpha and theta power summarize EEG spectral content; HHT complexity provides a nonlinear characteristic of

nonstationary EEG activity. The extended set (M3) appended HER_frontal, a frontal heartbeat-evoked-response summary, and SDHR, an ECG-derived statistic of heart-rate dispersion. We fitted M2 and M3 to the same 121 individuals, avoiding the misleading comparison that would arise from changing the denominator between models.

We evaluated the selected microstate-coverage fields as a separate availability subset, not as part of the primary M3 comparison. Although the wider clinical concept involves qEEG, HHT, HER, HRV, and microstates, the reported M3 AUCs must not be described as performance of a model containing all five domains. In particular, the earlier manuscript did not include relative gamma power and high-frequency HRV variables among these six predictors.

Conceptually, microstates may indicate large-scale cortical organization relevant to the recovery of consciousness and post-coma rehabilitation. Their value is hypothesis-generating here: the main 121-patient model contains no microstate predictors, and completeness for selected microstate features was limited to 104 individuals.

We infer no mechanism solely from predictive coefficients: HER may reflect neural reafference or contamination; SDHR can be influenced by ectopy, medication, and hemodynamics. We use the terms cortical and autonomic as physiological hypotheses rather than guarantees of source attribution.

Cross-validation, algorithm development and uncertainty

We retained three model-evaluation procedures: elastic-net regularized logistic regression, gradient boosting, and a nested-selection procedure that selected among candidate learning algorithms within the training partitions. For each feature set, we repeated outer five-fold cross-validation five times. We selected hyperparameters using inner-fold resampling, and averaged outer held-out predictions for each patient across repetitions. This design protects evaluation records from within-fold optimization; repetition improves stability but does not create five independent cohorts.

Area under the receiver operating characteristic curve (AUC) measured discrimination, and Brier score summarized mean squared prediction error. We calculated the ROC curves from averaged patient-level out-of-fold probabilities, treating poor neurological outcome as the positive class for display. We compared M2 and M3 on paired patients. We generated exploratory 95% uncertainty intervals by stratified bootstrap resampling of the fixed averaged out-of-fold predictions, without retraining the full pipeline in each bootstrap sample.

Because we evaluated candidate algorithms and modeling choices on the same cohort, the highest algorithm-specific AUC may retain selection optimism even when we tuned individual hyperparameters within folds. The nested-selection result is therefore distinguished from the observed gradient-boosting benchmark. An interval for the change in AUC overlapping zero is not evidence of a confirmed incremental gain. We did not reconstruct DeLong P values, adjusted clinical odds ratios, multiple-

imputation models, exact specificity-threshold performance or an externally validated clinical score from the former manuscript [8,9,10,33,34].

Data governance, ethics and reproducibility

The source I-CARE recordings were de-identified and distributed under repository-specific conditions. Access arrangements differ across releases; authors must confirm the terms applicable to the files used, including restrictions associated with the Brain Data Science Platform and any prior access or re-use permissions. This report does not redistribute identifiable patient-level information or source EEG/ECG files.

Ethics approval

or exemption for the present secondary analysis, any applicable informed-consent waiver, and the precise authorizations governing previously downloaded or derived I-CARE data must be documented before submission. The derived tables alone cannot establish those permissions. Full code and non-restricted aggregate outputs should be made available where permitted, whereas restricted data must not be redistributed without explicit authorization. The IRB of the Institute of Neurology and Neurosurgery, Havana, approved this protocol.

RESULTS

Patient selection and biomarker availability

The analytical cohort comprised 134 coma records with known outcomes: 52 favorable (38.8%) and 82 poor (61.2%). Six-feature completeness was available for 121 records: 48 favorable (39.7%) and 73 poor (60.3%). Among these, 104 also had selected microstate coverage fields (43 favorable, 61 poor). The reduction from 134 to 121 reflects 13 records with at least one missing M3 predictor; an additional 17 records lacked at least one additional microstate feature. Figure 1 shows the availability flow, and Table 1 summarizes the cohort.

Table 1
Analytical cohorts and predictor availability.

Analytical cohort	N	Favorable	Poor	Predictor availability
Available coma records	134	52	82	Outcome available
M3 complete cases	121	48	73	Age, alpha, theta, HHT, frontal HER, SDHR
M3 + selected microstates	104	43	61	M3 variables + selected microstate coverage

Note. Cohort sizes describe feature availability. Specific causes of missing measurements were not independently verified.

Internally cross-validated discrimination and prediction error

All comparisons in the principal model analysis used the same 121 patients. Elastic net yielded AUC 0.6438 for M2 (fixed-prediction 95% interval 0.5342–0.7420) and AUC 0.7055 for M3 (0.6118–0.7925), with Brier scores 0.2213 and 0.2083. Gradient boosting yielded AUC 0.7126 for M2 (0.6204–0.8008) and 0.7377 for M3 (0.6443–0.8308); corresponding Brier scores were 0.2116 and 0.1970.

When learning-algorithm selection was conducted within the nested procedure, M2 AUC was 0.6541 (0.5456–0.7512), and M3 AUC was 0.7092 (0.6138–0.7982), with Brier scores of 0.2156 and 0.2073. The numerically strongest M3 result was the algorithm-specific gradient-boosting AUC of approximately 0.74, whereas the procedure incorporating within-fold algorithm selection attained approximately 0.71. These results describe internal exploratory performance, not performance in an independent hospital cohort (Fig. 3, Fig. 4 and Table 2).

Table 2
Internally cross-validated discrimination and prediction error.

Algorithm	Model	N	AUC	95% CI*	Brier
Elastic Net	M2	121	0.6438	0.5342 to 0.7420	0.2213
Elastic Net	M3	121	0.7055	0.6118 to 0.7925	0.2083
Gradient Boosting	M2	121	0.7126	0.6204 to 0.8008	0.2116
Gradient Boosting	M3	121	0.7377	0.6443 to 0.8308	0.1970
Nested selection	M2	121	0.6541	0.5456 to 0.7512	0.2156
Nested selection	M3	121	0.7092	0.6138 to 0.7982	0.2073

*Note. *Exploratory stratified bootstrap intervals conditional on fixed averaged out-of-fold predictions. Model refitting is not included.*

Table 2
Internally cross-validated predictive performance

Algorithm	Model	N	AUC	95% CI*	Brier
Elastic Net	M2	121	0.6438	0.5342 to 0.7420	0.2213
Elastic Net	M3	121	0.7055	0.6118 to 0.7925	0.2083
Gradient Boosting	M2	121	0.7126	0.6204 to 0.8008	0.2116
Gradient Boosting	M3	121	0.7377	0.6443 to 0.8308	0.1970
Nested selection	M2	121	0.6541	0.5456 to 0.7512	0.2156
Nested selection	M3	121	0.7092	0.6138 to 0.7982	0.2073

*Note. *Exploratory stratified bootstrap intervals conditional on fixed averaged out-of-fold predictions. Model refitting is not included.*

Patient-level separation and overlap

Empirical ROCs were calculated from averaged out-of-fold predictions rather than smoothed or synthetic patient scores. The gradient-boosting M3 probability display shows a tendency toward higher predicted probability of poor outcome among patients with poor outcomes, alongside considerable overlap with the favorable group. The individual scatter points in Fig. 5 correspond to held-out predictions; horizontal jitter was added only to distinguish overlapping points. The figure is descriptive and does not define a safe threshold for withdrawal of life-sustaining therapy.

Incremental association of HER and HRV with predictive discrimination

The six-feature M3 model produced positive numerical AUC changes relative to M2 with all three methods: +0.0616 for elastic net (95% interval − 0.0052 to + 0.1390), + 0.0251 for gradient boosting (− 0.0511 to + 0.1045) and + 0.0551 for nested selection (− 0.0220 to + 0.1347). Each interval crossed zero. The results are compatible with modest benefit but also with no incremental benefit under the current analysis and uncertainty assumptions (Fig. 6 and Table 3).

Table 3
Paired incremental discrimination after adding HER and HRV.

Algorithm	Delta AUC	95% CI*	Brier M2	Brier M3
Elastic Net	+ 0.0616	-0.0052 to 0.1390	0.2213	0.2083
Gradient Boosting	+ 0.0251	-0.0511 to 0.1045	0.2116	0.1970
Nested selection	+ 0.0551	-0.0220 to 0.1347	0.2156	0.2073

*Note. *Exploratory fixed-prediction bootstrap confidence intervals. An incremental improvement has not been established with confirmatory statistical evidence.*

Table 3
Incremental value of HER and HRV

Algorithm	Delta AUC	95% CI*	Brier M2	Brier M3
Elastic Net	+ 0.0616	-0.0052 to 0.1390	0.2213	0.2083
Gradient Boosting	+ 0.0251	-0.0511 to 0.1045	0.2116	0.1970
Nested selection	+ 0.0551	-0.0220 to 0.1347	0.2156	0.2073

*Note. *Exploratory fixed-prediction bootstrap confidence intervals. An incremental improvement has not been established with confirmatory statistical evidence.*

Across methods, Brier scores were lower for M3 than M2, which suggests a numerical reduction in prediction error. Nevertheless, fixed-prediction resampling and the absence of external calibration testing limit this finding; we did not infer clinically meaningful calibration improvement from Brier scores alone.

DISCUSSION

The principal scientific contribution is a multimodal framework bringing together complementary aspects of cerebral electrophysiology and cardiovascular regulation after cardiac arrest. Spectral EEG measures, nonlinear complexity, heartbeat-evoked responses, and heart-rate variability probe distinct yet potentially interacting dimensions of post-anoxic dysfunction. Together, they allow a broader physiological assessment than an isolated EEG or ECG marker, though the observed outcome discrimination remains exploratory.

Recovery from coma depends on more than the persistence of isolated cortical rhythms. It requires functional integrity and reorganization of distributed neuronal systems and their interactions with subcortical and autonomic networks. Cortical spectral power and Hilbert-Huang complexity describe different characteristics of cerebral activity; frontal heartbeat-evoked responses and cardiac interval dynamics offer complementary views of brain-heart coupling. These physiological interpretations are hypotheses, not proof of a specific neural source or mechanism.

A distinctive methodological strength is expert-supervised signal curation. The corresponding author (C.M.), an experienced clinical neurophysiologist, personally visually reviewed EEG/ECG and incorporated independent component analysis when preparing the derived features. Such clinical scrutiny helps identify artifacts, extracranial contributions, and rhythm disturbances that automated extraction alone may misinterpret. This contribution strengthens the use of shared physiological repositories without making the database origin the central scientific finding.

Comparing four and six predictors provides a transparent test of the biological premise. Age and EEG-derived spectral and nonlinear features characterize clinical context and cortical physiology. Frontal HER and SDHR may add information about neurovisceral interactions after global ischemia, a plausible process given injury effects on interoception and brainstem–cortical regulation [21,22,23,24]. However, the meaning of a frontal R-locked voltage depends on its relationship to ECG waveform morphology, component separation, and surrogate heartbeat timing. Similarly, SDHR alone does not identify sympathetic or parasympathetic tone, particularly in critically ill patients receiving multiple drugs [25,26,27,28].

The highest observed AUC of 0.7377 was obtained with gradient boosting using the six-feature set. Yet the difference relative to the four-feature gradient-boosting model was only 0.0251, and its fixed-prediction bootstrap interval included zero. Elastic net showed a larger numerical difference, but its lower confidence bound was also just below zero. The nested-selection comparison likewise failed to exclude no improvement. These convergent results suggest that any net gain is small, unstable, or currently uncertain, rather than demonstrating a robust independent HER/HRV effect.

Moreover, a large AUC does not imply safety for bedside neuroprognostication. In this setting, a false-positive prediction of poor outcome may influence withdrawal of potentially beneficial treatment. Reliable models should undergo external testing, calibration assessment, and validation at prespecified high-specificity thresholds under appropriate timing and sedation conditions. Earlier reports of 96.2% specificity, adjusted odds ratios, or a DeLong P value from a different analytical pipeline cannot be transferred to the models evaluated here [1,2,4,5,9,35].

Although multimodal neurophysiological monitoring can provide valuable information for neurological prognostication after cardiac arrest, physicians must recognize that **prognosis remains an individualized clinical judgment made at the patient's bedside**. Predictive models and electrophysiological biomarkers should complement, rather than replace, comprehensive clinical assessment. Physicians must carefully consider each patient's neurological examination, medical history, comorbidities, sedation and other potential confounders, clinical course over time, and overall condition. Pay particular attention to the dynamic nature of neurological recovery, since early findings may not fully reflect an individual patient's potential for improvement. Therefore, prognostic decisions should be based on an integrated, patient-centered, and multidisciplinary evaluation, avoiding premature conclusions or irreversible decisions based solely on statistical probabilities. Ultimately, the physician's clinical expertise, direct observation,

and individualized assessment remain indispensable to responsible bedside neuroprognostication and patient-centered clinical decision-making [36].

EEG microstates offer a complementary description of the temporal organization of large-scale cortical electrical activity. Their coverage, duration, and transitions may reflect coordinated network processes potentially relevant to recovery of consciousness and post-coma functional rehabilitation. This neurobiological perspective warrants longitudinal investigation rather than a claim of demonstrated therapeutic or predictive utility. In the present data, selected microstate measures were complete in only 104 cases compared with 121 cases for the main EEG-ECG comparison. Consequently, the reported M3 AUC does not include microstates and cannot establish their incremental value. Prospective studies should investigate whether microstate trajectories complement spectral, nonlinear, and brain-heart biomarkers during recovery.

There are several limitations. *First*, this is a secondary analysis of stored features derived from only part of the I-CARE population. We could not fully reconstruct the reasons for including or excluding individual patients. *Second*, we did not have all source EEG/ECG traces and expert-annotation logs for this audit. *Third*, model comparison and algorithm exploration used the same sample, so selection optimism is possible despite internal cross-validation. *Fourth*, resampling intervals condition on fixed predictions and cannot capture uncertainty in model development and data cleaning. *Fifth*, the authors did not perform independent external validation.

The study also indicates a practical research standard for investigators working with open clinical biosignals: public availability should not be confused with either data-use authorization or physiological validity. Transparent inclusion rules dated access permissions, reproducible quality logs, expert-reviewed example traces, complete prediction files, and preplanned independent validation would make future reports more interpretable and more likely to merit editorial consideration. These requirements preserve the advantages of shared scientific infrastructure while meeting the responsibilities of clinical neuroprognostication.

In conclusion, expert-guided multimodal EEG-ECG integration provides a physiologically informed framework for studying cortical dynamics and brain-heart interactions after cardiac arrest. The six-feature model yielded moderate internal discrimination, with an exploratory Gradient Boosting AUC of 0.738, although the incremental contribution of HER and HRV was not statistically established. EEG microstates offer an additional hypothesis concerning network organization during recovery from coma but were not included in the primary predictive model. External validation, reproducible signal-quality documentation and confirmation of the applicable data-use permissions are necessary before clinical deployment.

Declarations

Ethics and consent: Authors must insert the exact ethics committee approvals or waivers and informed-consent justification covering the source consortium and this secondary analysis. Nonetheless, the IRB

of the Institute of Neurology and Neurosurgery, Havana, approved this research

Data access and permission: The project uses I-CARE-derived features. The authors must identify the release, acquisition date, terms of use, and written permissions applicable to their data access and to any restricted derivative files; sharing of restricted source records is not proposed.

Author Contributions

C.M.: Conceptualization, study design, methodology, data acquisition and curation, expert visual EEG–ECG inspection, independent component analysis (ICA), neurophysiological signal processing, multimodal feature extraction, statistical analysis, machine-learning modeling, validation, interpretation of results, visualization, and preparation of the original manuscript.

J.J.S., B.D.S., M.D., and R.M.: Verification of the manuscript's scientific content, critical review and editing of the manuscript, and final approval of the version submitted for publication.

All authors reviewed and approved the final manuscript and agreed to be accountable for their respective contributions.

Funding and competing interests: The authors declare no competing interests.

Code and materials: Analytic scripts and aggregate results may be shared subject to repository permissions. Do not redistribute patient-level source data and controlled-access derivatives without authorization.

Use of artificial intelligence: Generative AI tools were used only to assist with English grammar and language editing, preparing and debugging analysis and figure-production scripts, and formatting figures. AI was not used to generate or fabricate patient data, EEG or ECG recordings, clinical outcomes, measurements, or statistical results. All numerical results originate from analyses of the study data. The authors reviewed the outputs and remain fully responsible for the scientific content, analyses, and conclusions.

References

1. 1. Nolan JP, Sandroni C, Böttiger BW, et al. European Resuscitation Council and European Society of Intensive Care Medicine Guidelines 2021: Post-resuscitation care. Resuscitation. 2021;161:220–269.
2. 2. Nolan JP, Sandroni C, Böttiger BW, et al. European Resuscitation Council and European Society of Intensive Care Medicine guidelines 2021: post-resuscitation care. Intensive Care Med. 2021;47:369–421.

3. 3. Sandroni C, Cronberg T, Sekhon M. Brain injury after cardiac arrest: pathophysiology, treatment, and prognosis. Intensive Care Med. 2021;47:1393–1414.
4. 4. Rajajee V, Muehlschlegel S, Wartenberg KE, et al. Guidelines for neuroprognostication in comatose adult survivors of cardiac arrest. Neurocrit Care. 2023;38(3):533–563.
5. 5. Elmer J, Torres C, Aufderheide TP, et al. Association of early withdrawal of life-sustaining therapy for perceived neurological prognosis with mortality after cardiac arrest. Resuscitation. 2016;102:127–135.
6. 6. Amorim E, Zheng WL, Ghassemi MM, et al. The International Cardiac Arrest Research (I-CARE) Consortium Electroencephalography Database. Crit Care Med. 2023. doi:10.1097/CCM.0000000000006074.
7. 7. Goldberger AL, Amaral LAN, Glass L, et al. PhysioBank, PhysioToolkit, and PhysioNet: Components of a New Research Resource for Complex Physiologic Signals. Circulation. 2000;101:e215–e220.
8. 8. Topol EJ. High-performance medicine: The convergence of human and artificial intelligence. Nat Med. 2019;25:44–56.
9. 9. Geocadin RG, Callaway CW, Fink EL, et al. Standards for studies of neurological prognostication in comatose survivors of cardiac arrest: A scientific statement from the American Heart Association. Circulation. 2019;140(9):e517–e542.
10. 10. Collins GS, Moons KGM, Dhiman P, et al. TRIPOD + AI statement: updated guidance for reporting clinical prediction models that use artificial intelligence. BMJ. 2024;385:e078378.
11. 11. Ruijter BJ, Tjepkema-Cloostermans MC, Tromp SC, et al. Early electroencephalography for outcome prediction of postanoxic coma: a prospective cohort study. Ann Neurol. 2019;86:203–214.
12. 12. Sandroni C, Grippo A, Nolan JP. ERC–ESICM guidelines for prognostication after cardiac arrest: time for an update. Intensive Care Med. 2020;46:1901–1903.
13. 13. Drohan CM, Cardi AI, Rittenberger JC, et al. Effect of sedation on quantitative electroencephalography after cardiac arrest. Resuscitation. 2018;124:132–137.
14. 14. Lamartine Monteiro M, Taccone FS, Depondt C, et al. The prognostic value of 48-h continuous EEG during therapeutic hypothermia after cardiac arrest. Neurocrit Care. 2016;24:153–162.
15. 15. Beuchat I, Solari D, Novy J, Oddo M, Rossetti AO. Standardized EEG interpretation in patients after cardiac arrest: correlation with other prognostic predictors. Resuscitation. 2018;126:143–146.
16. 16. Benarous L, Gavaret M, Soda Diop M, et al. Sources of interrater variability and prognostic value of standardized EEG features in post-anoxic coma after resuscitated cardiac arrest. Clin Neurophysiol Pract. 2019;4:20–26.
17. 17. Caporro M, Rossetti AO, Seiler A, et al. Electromyographic reactivity measured with scalp EEG contributes to prognostication after cardiac arrest. Resuscitation. 2019;138:146–152.
18. 18. Hofmeijer J, Tjepkema-Cloostermans MC, van Putten MJAM. Burst-suppression with identical bursts: a distinct EEG pattern with poor outcome in post-anoxic coma. Clin Neurophysiol.

2014;125:947–954.

19. 19. Admiraal MM, van Rootselaar AF, Horn J, et al. Electroencephalographic reactivity as predictor of neurological outcome in postanoxic coma: A multicenter prospective cohort study. Ann Neurol. 2019;86(1):17–27.
20. 20. Huang NE, Wu Z. A review on Hilbert–Huang transform: Method and its applications. Rev Geophys. 2008;46:RG2006.
21. 21. Candia-Rivera D, Machado C. Reduced heartbeat-evoked responses in a near-death case report. J Clin Neurol. 2023;19(6):581–588.
22. 22. Candia-Rivera D, Machado C. Multidimensional assessment of heartbeat-evoked responses in disorders of consciousness. Eur J Neurosci. 2023;58(4):3098–3110.
23. 23. Candia-Rivera D, Raimondo F, Pérez P, et al. Conscious processing of global and local auditory irregularities causes differentiated heartbeat-evoked responses. eLife. 2023;12:e75352.
24. 24. Park G, Blanke O. Coupling inner and outer body for self-consciousness. Trends Cogn Sci. 2019;23:377–388.
25. 25. Shaffer F, Ginsberg JP. An overview of heart rate variability metrics and norms. Front Public Health. 2017;5:258.
26. 26. Task Force of the European Society of Cardiology. Heart rate variability: Standards of measurement, physiological interpretation and clinical use. Circulation. 1996;93:1043–1065.
27. 27. Kuo TBJ, Yang CCH, Huang NE. Quantification of respiratory sinus arrhythmia using Hilbert–Huang transform. Adv Adapt Data Anal. 2009;1:295–307.
28. 28. Li H, Kwong S, Yang L, et al. Application of Hilbert–Huang transform for nonlinear analysis of heart rate variability. IEEE/ACM Trans Comput Biol Bioinform. 2011;8:1557–1567.
29. 29. Michel CM, Koenig T. EEG microstates as a tool for studying the temporal dynamics of whole-brain neuronal networks: A review. NeuroImage. 2018;180:577–593.
30. 30. Khanna A, Pascual-Leone A, Michel CM, Farzan F. Microstates in resting-state EEG: Current status and future directions. Neurosci Biobehav Rev. 2015;49:105–113.
31. 31. Catrambone V, Valenza G. Towards the definition of microstates of the cortical brain-heart axis. Proc Annu Int Conf IEEE Eng Med Biol Soc. 2023:10340338.
32. 32. Britz J, Van De Ville D, Michel CM. BOLD correlates of EEG topography reveal rapid resting-state network dynamics. Proc Natl Acad Sci USA. 2010;107:18125–18130.
33. 33. Andersson P, Johnsson J, Björnsson O, et al. Predicting neurological outcome after out-of-hospital cardiac arrest with cumulative information: development and internal validation of an artificial neural network algorithm. Crit Care. 2021;25:83.
34. 34. Kim TJ, Suh J, Park SH, et al. System for predicting neurological outcomes following cardiac arrest based on clinical predictors using a machine learning method: The Neurological Outcomes After Cardiac Arrest (NOCA) method. Neurocrit Care. 2025;42(3):829–838.
35. 35. Sandroni C, D'Arrigo S, Nolan JP. Prognostication after cardiac arrest. Crit Care. 2018;22:150.

36. 36. Machado C. The Controversial Case of Jahi McMath: The Reality of a Suspected Brain-Dead Patient. Newcastle upon Tyne: Cambridge Scholars Publishing; 2026. ISBN: 978-1-0364-6864-4.

Figures

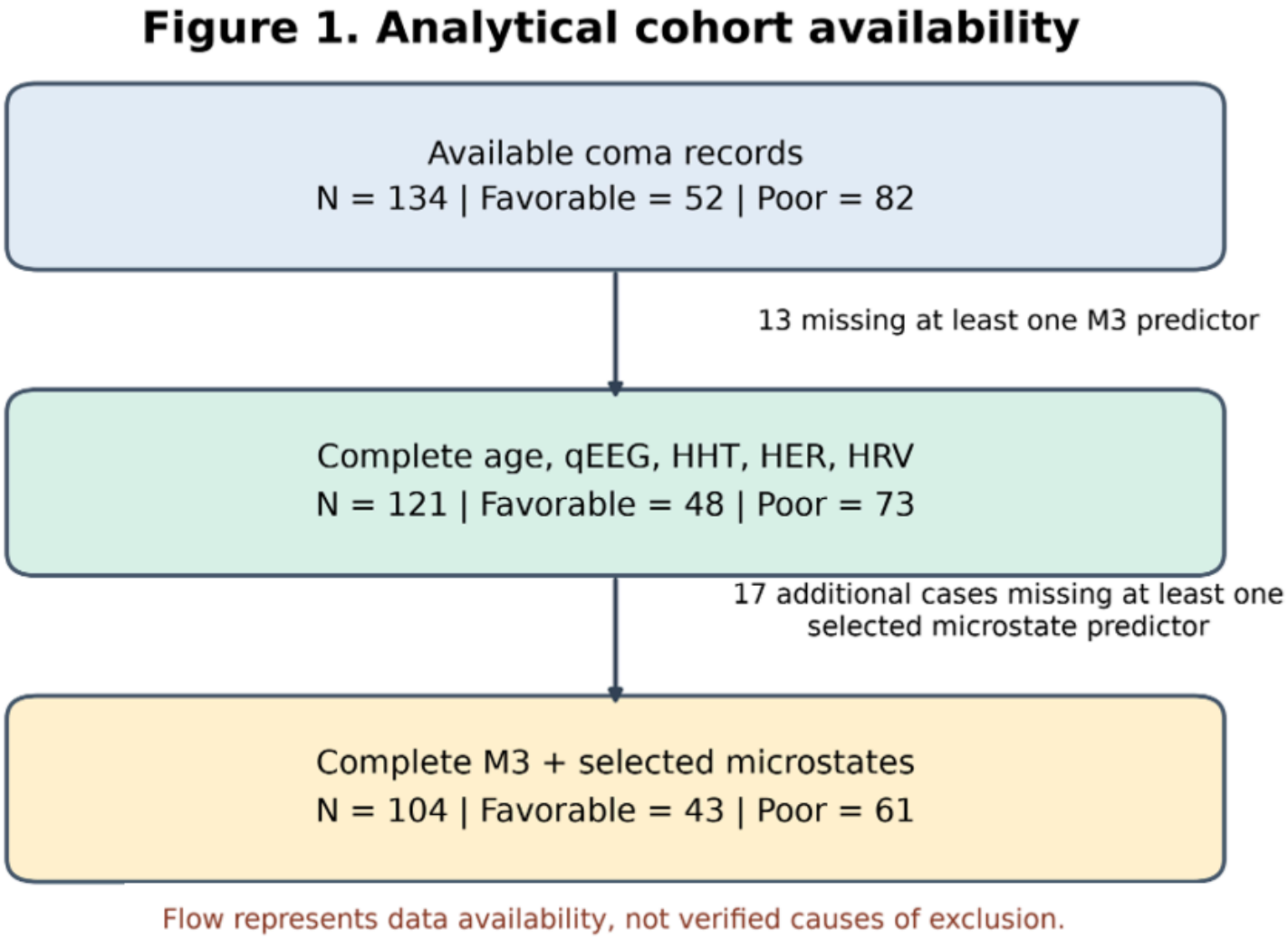


Figure 1

Analytical cohort availability for multimodal neurophysiological assessment. The initial cohort comprised 134 post-cardiac-arrest patients with available neurological outcomes. Complete EEG, HHT, HER, HRV, and age-derived predictors were available for 121 patients, while 104 additionally had complete selected EEG microstate measures. The diagram represents analytical data availability rather than the original screening process.

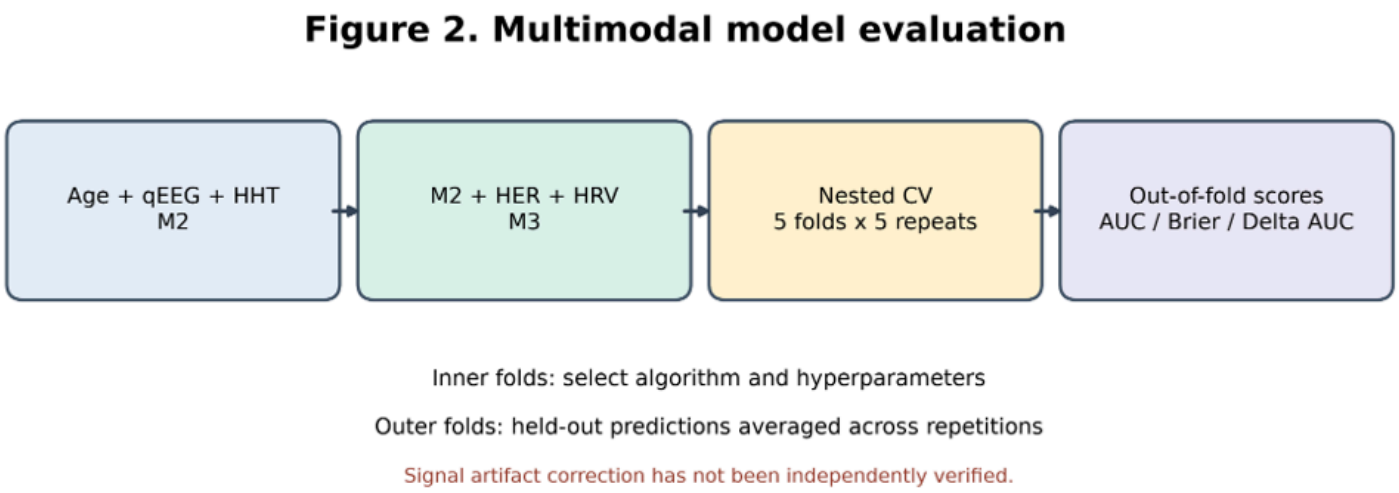


Figure 2

Expert-guided multimodal EEG–ECG integration and predictive modeling workflow. Schematic representation of the parallel evaluation of two complementary neurophysiological predictor sets in 121 post-cardiac-arrest patients. Model M2 incorporated age, quantitative EEG relative alpha and theta power, and Hilbert–Huang transform (HHT) complexity, reflecting clinical context, cortical spectral organization, and nonlinear cerebral dynamics. Model M3 additionally integrated frontal heartbeat-evoked responses (HERs) and heart rate variability (SDHR), providing complementary information on brain–heart interactions and cardiovascular regulation. Both models underwent repeated nested five-fold cross-validation (five repetitions), with algorithm and hyperparameter selection performed within the inner training folds. Predictive discrimination and accuracy were assessed using averaged out-of-fold predictions, area under the receiver operating characteristic curve (AUC), Brier score, and paired differences in AUC.

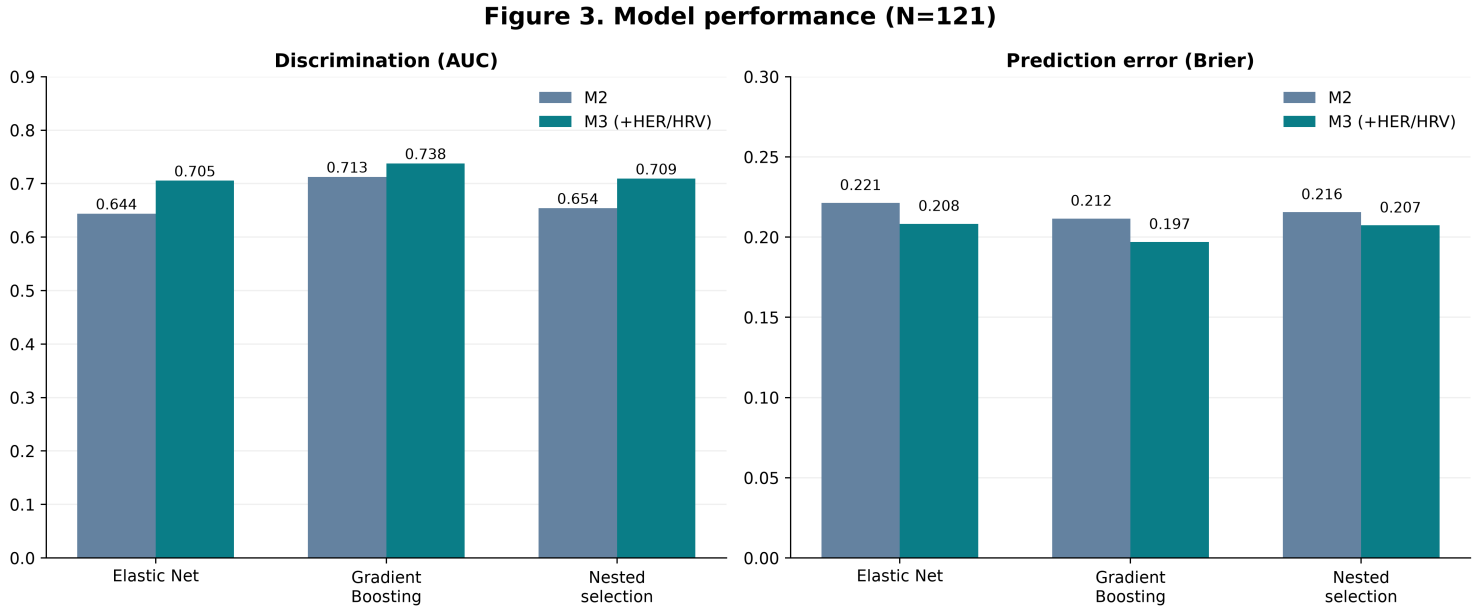


Figure 3

significant incremental predictive value of HER and HRV.Comparative predictive performance of multimodal neurophysiological models after cardiac arrest. Comparison of discrimination (left panel), expressed as the area under the receiver operating characteristic curve (AUC), and prediction error (right panel), quantified using the Brier score, across three machine-learning approaches: Elastic Net, Gradient Boosting, and nested algorithm selection. Two predictor sets were evaluated in the same 121 post-cardiac-arrest patients: M2 combined age, relative alpha and theta EEG power, and Hilbert–Huang transform (HHT) complexity, whereas M3 additionally incorporated frontal heartbeat-evoked responses (HERs) and heart rate variability (SDHR), representing complementary aspects of cortical dynamics and brain–heart interactions. M3 showed higher AUCs and lower Brier scores across all three approaches, with Gradient Boosting achieving the highest AUC (0.738). We derived performance estimates from averaged out-of-fold predictions obtained through repeated nested five-fold cross-validation. Lower Brier scores indicate lower prediction error. The observed improvements were exploratory and do not establish statistically

Figure 4. Empirical out-of-fold ROC curves

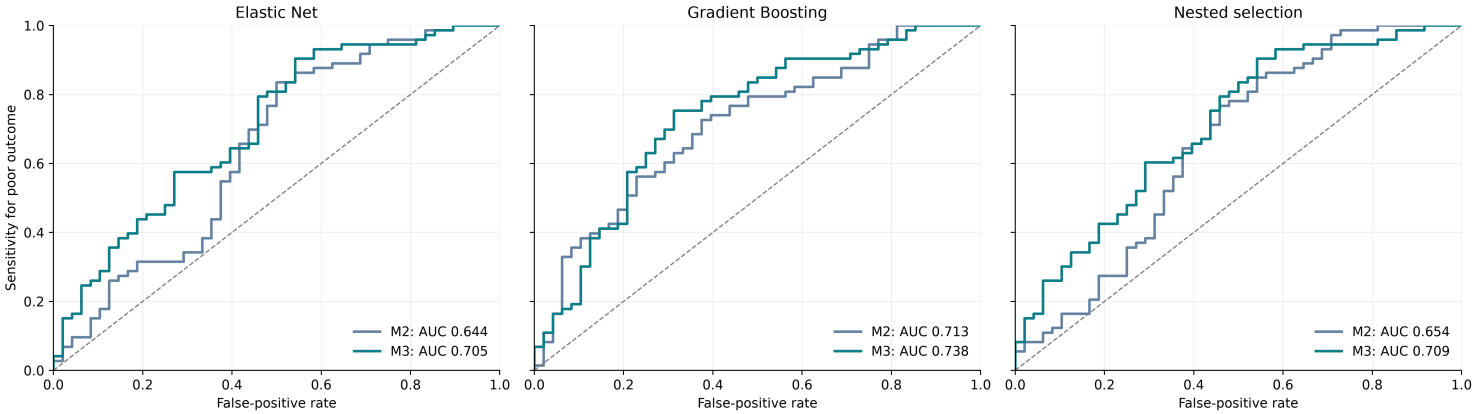


Figure 4

Empirical out-of-fold receiver operating characteristic (ROC) curves of multimodal neurophysiological models for neurological outcome prediction after cardiac arrest. ROC curves compare the discriminative performance of two predictor sets across three machine-learning approaches: Elastic Net (left panel), Gradient Boosting (middle panel), and nested algorithm selection (right panel). Model M2 incorporated age, relative alpha and theta EEG power, and Hilbert–Huang transform (HHT) complexity, whereas M3 additionally integrated frontal heartbeat-evoked responses (HERs) and heart rate variability (SDHR), representing complementary cortical and brain–heart physiological domains. We evaluated all models in the same 121 post-cardiac-arrest patients using repeated nested five-fold cross-validation, with ROC curves derived from averaged out-of-fold predictions. We defined poor neurological outcome (CPC 3–5) as the positive class. The dashed diagonal represents chance-level discrimination (AUC = 0.50). M3 achieved higher AUCs than M2 across all three approaches, with the highest observed discrimination obtained using Gradient Boosting (AUC = 0.738). These findings indicate moderate exploratory predictive performance, while the incremental contribution of HER and HRV remains statistically uncertain.

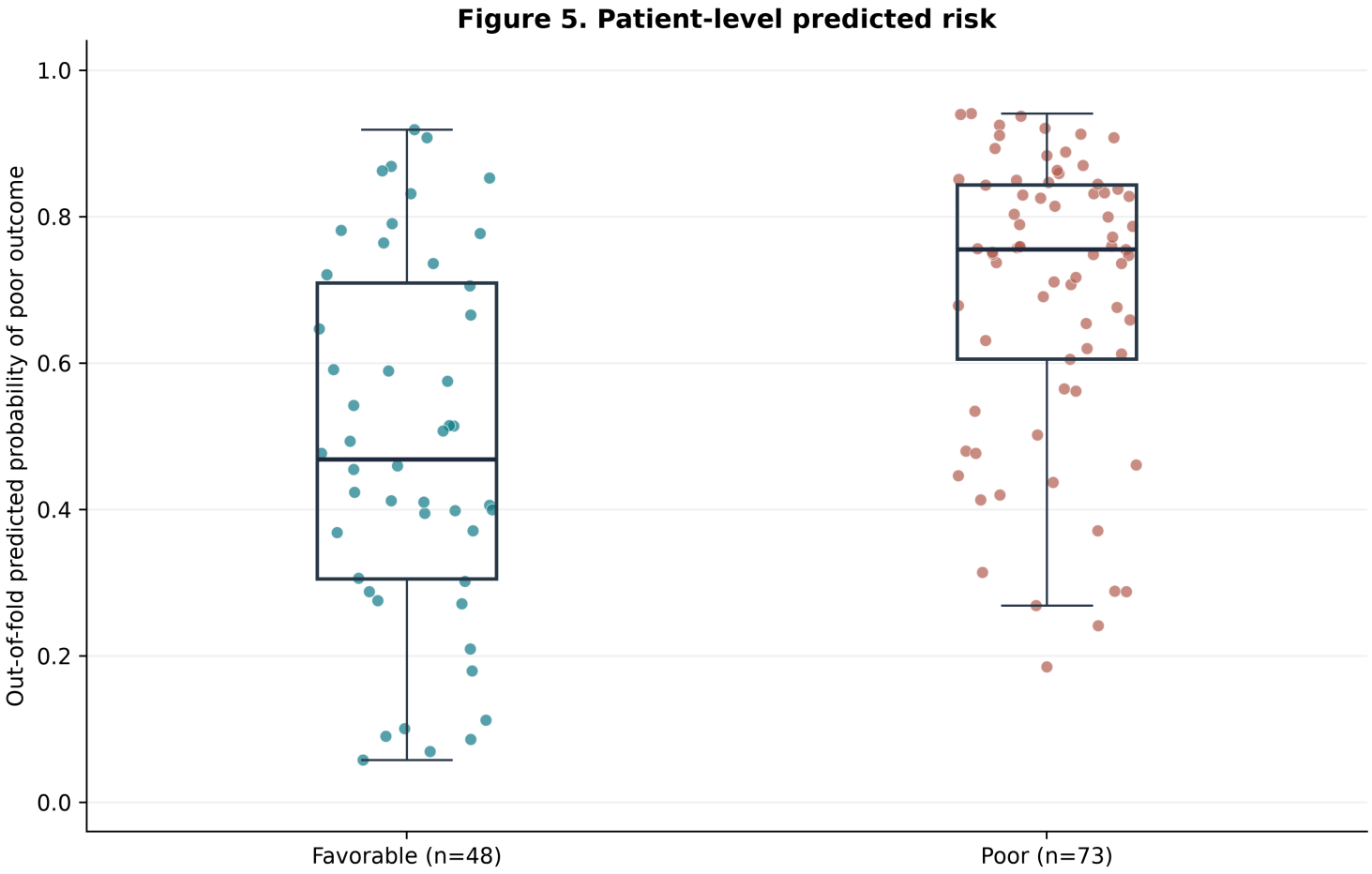


Figure 5

Patient-level distribution of predicted neurological outcome risk derived from expert-guided multimodal EEG–ECG integration after cardiac arrest. Box-and-scatter plots illustrate the distribution of out-of-fold predicted probabilities of poor neurological outcome (Cerebral Performance Category [CPC] 3–5) generated by the six-feature Gradient Boosting model (M3) in 121 post-cardiac-arrest patients. The model integrated age, relative alpha and theta EEG power, Hilbert–Huang transform (HHT) complexity, frontal heartbeat-evoked responses (HERs), and heart rate variability (SDHR), combining complementary measures of cortical dynamics and brain–heart interactions. We grouped patients by observed neurological outcomes: favorable (CPC 1–2; n = 48) and poor (CPC 3–5; n = 73). Each dot represents an individual patient's averaged out-of-fold predicted probability obtained through repeated nested five-fold cross-validation; horizontal jitter was applied solely for visualization. Boxes indicate the interquartile range, horizontal lines represent the median, and whiskers extend to the most extreme observations within 1.5 times the interquartile range. Predicted risk was generally higher in the poor-outcome group, although substantial overlap was observed between groups. These findings illustrate moderate internal discrimination rather than an externally validated clinical decision threshold.

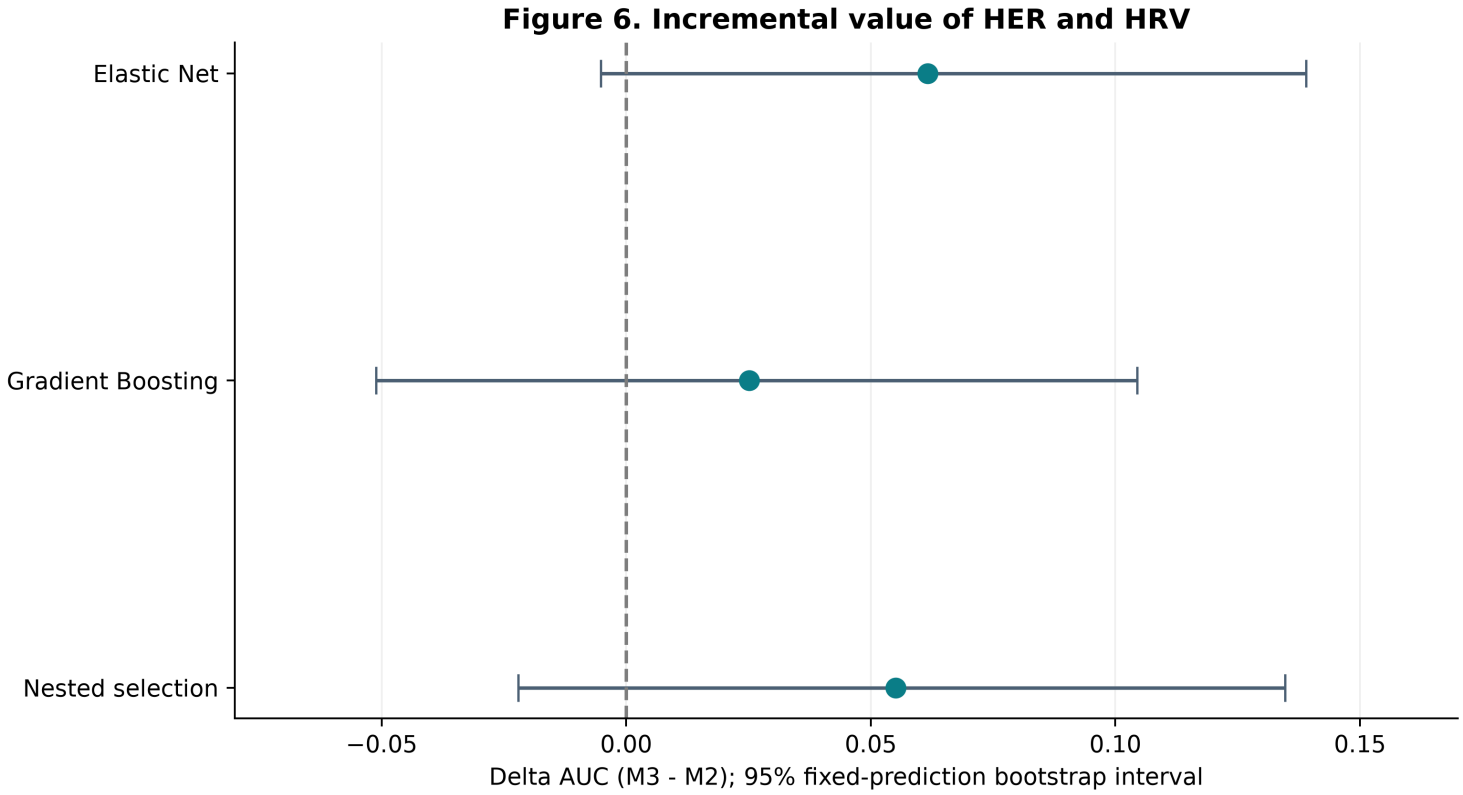


Figure 6

Incremental predictive contribution of heartbeat-evoked responses and heart rate variability to multimodal neurological outcome prediction after cardiac arrest. Forest plot illustrating paired differences in the area under the receiver operating characteristic curve (ΔAUC) between the six-feature multimodal model (M3) and the four-feature baseline model (M2) across three machine-learning approaches: Elastic Net, Gradient Boosting, and nested algorithm selection. M2 incorporated age, relative alpha and theta EEG power, and Hilbert–Huang transform (HHT) complexity, whereas M3 additionally integrated frontal heartbeat-evoked responses (HERs) and heart rate variability (SDHR), representing complementary aspects of cortical dynamics and brain–heart interactions. All comparisons used the same 121 post-cardiac-arrest patients and were based on averaged out-of-fold predictions from repeated nested five-fold cross-validation. Dots represent observed ΔAUC estimates: +0.0616 for Elastic Net, +0.0251 for Gradient Boosting, and +0.0551 for nested selection. Horizontal error bars indicate exploratory 95% bootstrap confidence intervals conditional on fixed out-of-fold predictions, without model refitting. The dashed vertical line represents no incremental discrimination (ΔAUC = 0). Although all three approaches showed numerical improvements after incorporating HER and HRV, every confidence interval crossed zero, indicating that we did not establish a statistically conclusive incremental predictive benefit.